Chapter 9
Liquid Crystals for Organic Field-Effect Transistors

Mary O'Neill and Stephen M. Kelly

9.1   Introduction

Organic semiconductors are becoming a viable alternative to amorphous silicon for a range of thin film transistor devices. Indeed, plastic and organic electronics are considered disruptive technologies enabling new applications including intelligent or interactive packaging, RFID tags, e-readers, flexible power sources and lighting panels. The future success of the industry depends on the availability of high performance, solution-processable, materials for low cost manufacturing as well as low voltage device operation. The organic field effect transistor (OFET) is the fundamental building block of plastic electronics and is used to amplify and switch electronic signals. The key figure of merit for OFETs is the charge carrier mobility, (μ), the hole/electron velocity per unit field. Carrier transport occurs by hopping via π-π interactions between sites, which may be traps, single molecules, several repeat units of a polymer chain or even a number of delocalised chain segments in high-mobility conjugated mainchain polymers. There has been excellent progress in the development of solution processed organic semiconductors for OFETs [1–3]. The state-of-the-art performance is now equivalent to that of amorphous silicon.

M. O'Neill (✉)
Department of Physics and Mathematics, University of Hull, Hull, HU6 7RX UK
e-mail: m.oneill@hull.ac.uk

S.M. Kelly
Department of Chemistry, University of Hull, Hull, HU6 7RX UK
e-mail: s.m.kelly@hull.ac.uk

9.2 Principle of Organic Field-Effect Transistors

Transistors are organic semiconductor devices used to amplify and switch electronic signals. In an organic field-effect transistor (OFET) a voltage applied to the gate electrode controls the current between the source and drain electrodes [4, 5]. The construction of a typical OFET is shown in Fig. 9.1. An insulator is placed between the gate and the organic semiconducting thin film. The source and drain electrode are separated by a semiconducting channel of length L and width W. Ideally, when no gate voltage, V_G, is applied, the conductance of the semiconductor film is extremely low, because there are no mobile charge carriers, i.e., the device is "off". The application of V_G gives an electric field across the dielectric, which induces mobile charges in the semiconductor film. These move in response to the voltage, V_D, applied between the source and drain, i.e., the transistor is "on". Figure 9.1 is an example of a bottom-gate, top-contact device configuration. The source and drain electrodes may be deposited between the dielectric and semiconducting thin film giving a bottom-gate, bottom-contact device. Alternatively the layers can be applied sequentially in the order: source and drain electrodes, semiconducting thin film, insulator and gate electrode giving a top-gate configuration. Figure 9.1 also show the circuit used to test the OFET. The source electrode is placed at ground. A hole drain current, I_D, is measured when a negative V_G is applied, as illustrated in Fig. 9.1. The electron drain current is measured when a positive V_G is applied. V_G must be greater than a threshold value V_T, before current flows because the contacts may not be ohmic and charge-carrier traps must first be filled. Figure 9.2 shows the output characteristic curve of the transistor, i.e., a plot of I_D versus V_D for different values of V_G. Two regions of the characteristic curve can be differentiated: I_D increases approximately linearly for low values of V_D, is when $V_D << (V_G - V_T)$. When $(V_G - V_T) > V_D$, I_D saturates. The physics underlying these characteristics is beyond the scope of this volume and is well explained elsewhere [5].
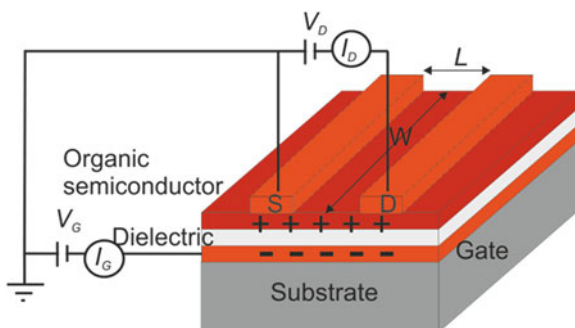

Fig. 9.1 Schematic of an OFET. The gate electrode is deposited on a substrate. The dielectric layer and p-type organic semiconducting film are deposited sequentially on top. The source S and drain D electrodes are photo lithographically patterned to define a channel of width W and length L. The gate and drain voltages are V_G and V_D respectively with corresponding notation for current I

Fig. 9.2 Output characteristics of a typical OFET showing I_D versus V_D plotted for different values of V_G. At low voltages, there is an approximate linear change of I_D with V_D. The current saturates at higher voltages
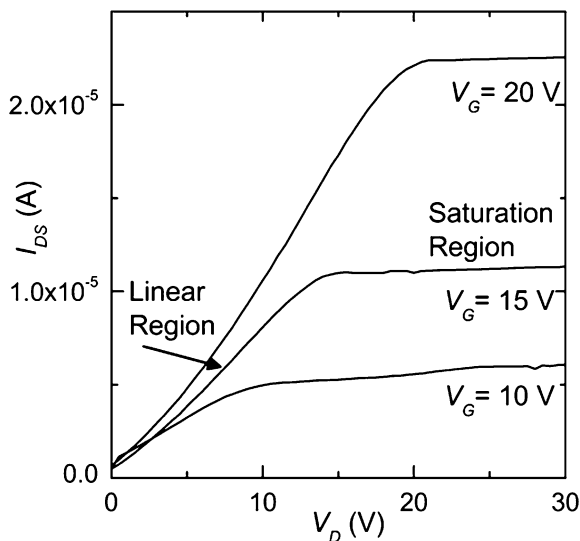
The charge-carrier mobility μ_{FET} is a key parameter obtained from the characteristics. It can be determined from the linear region using the equation

$$I_D = \frac{WC}{L}\mu_{FET}\left[(V_G - V_T)\,V_D - V_D{}^2\right] \tag{9.1}$$

where C is the capacitance per unit area of the insulator. Alternatively, keeping V_D constant in the saturation region, μ_{FET} can be calculated from a plot of I_D versus $(V_G - V_T)^2$ using the equation

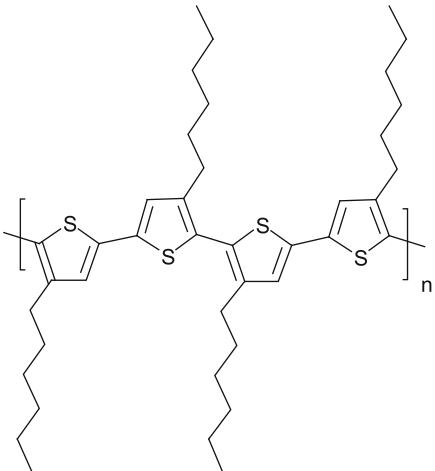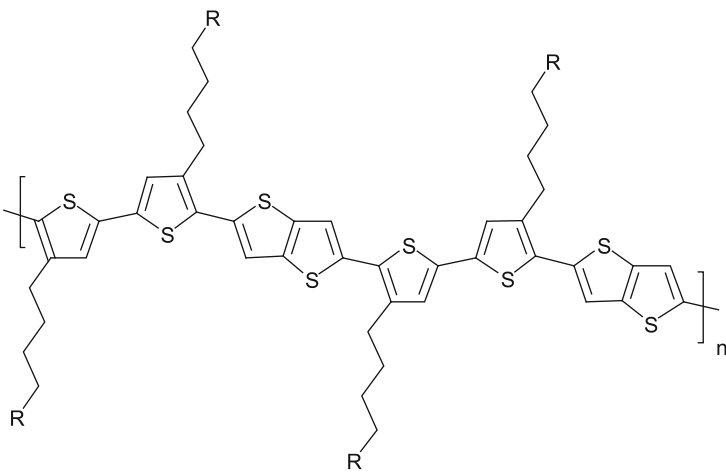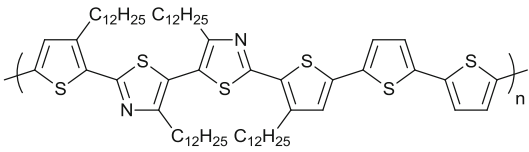$$I_D = \frac{WC}{L}\mu_{FET}(V_G - V_T)^2 \tag{9.2}$$

It is desired to maximise the magnitude of μ_{FET} so that the operating voltage and power consumption of the transistor can be minimised. Another important parameter is the on/off ratio, equal to I_D (on)/I_D (off) which should be sufficiently large to define the states "0" and "1" in electronic circuits.

9.3 Polymer Liquid Crystals for OFETs

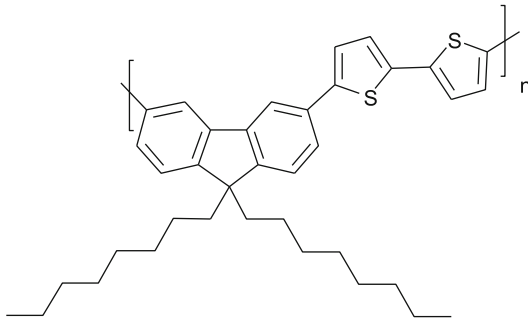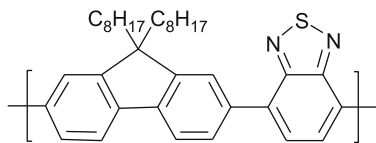### 9.3.1 Lamellar Polymers with High Temperature Smectic Phases

Before 2005 the bench-mark prototype semiconducting polymer was regioregular poly(3-hexylthiophene), compound **1** (P3HT), which shows hole mobility values of up to 0.3 cm^2 V^{-1} s^{-1} [2, 6]. Its chemical structure is shown in Table 9.1. Polymer **1**

Table 9.1 Chemical structures and phase transition temperatures of some liquid crystalline polymers

1

P3HT: $t_g \approx 67\ ^oC$; Cr-I $\approx 238\ ^oC$

2

PBTTT: Cr-SmX $\approx 171\ ^oC$; SmX-I $\approx 251\ ^oC$ [R = C_6H_{13}]

3

Sanditic polymer

Table 9.1 (continued)

4

F8T2: Cr-N ≈ 265 °C; N-I > 300 °C

5

F8BT: t_g ≈ 125-135 °C; Cr-N ≈ 258-283 °C; N-I > 300 °C

has a microcrystalline, lamellar structure, as shown in Fig. 9.3, consisting of closely-spaced layers of stacked, highly conjugated, aromatic backbones separated by layers of solubilising and insulating side chains, which facilitate large π-π coupling between adjacent polymers in the x direction because of the small separation between them. The insulating side-chains inhibit charge transport in the y direction. In-plane carrier transport is enhanced when the polymers adopt an an edge-on orientation on the surface as shown in the Fig. 9.3 and charge transport between segments of the same conjugated polymer chain is fast. However, the observed values of the charge carrier mobility can vary by orders of magnitude depending on the molecular weight and microcrystalline morphology of the polymer [7–9]. This variation may be due to poor interconnectivity between microcrystalline domains.

An excellent demonstration of the benefits of the self-assembly properties of liquid crystalline phases lies in the recent development of liquid crystalline, semiconducting, thiophene polymers and copolymers, many of which contain thienothiophene groups [11–17], see polymer **2**, poly(2,5-bis(3-alkylthiophen-2-yl)thieno [3,2-b]thiophene) (pBTTT), for example, which exhibits exceptionally high field-effect values of mobility up to 1 cm^2 V^{-1} s^{-1}. Such polymers possess a mesophase above room temperature associated with a lower side-chain density than polymer **1**, where each thiophene ring is substituted with an alkyl group. The lower density allows interdigitation, as illustrated in Fig. 9.4, and the mesophase corresponds to a highly-ordered smectic or saniditic phase of π-stacked backbones separated by melted and interdigitated aliphatic, non-conducting side-chains

Fig. 9.3 (**a**) Schematic illustration of charge transport modes in a lamella packed polymer assembly. *Rectangular units* denote monomers of the polymer backbone. *x* represents charge transport direction along the polymer chain, *z* between neighbouring chains with the backbones face-to-face, and *y* along the alkyl chains. (**b**) Schematic presentation of the π-stacking and the chain to chain packing of polymers. Reproduced from Ref. [10] with permission from The Royal Society of Chemistry
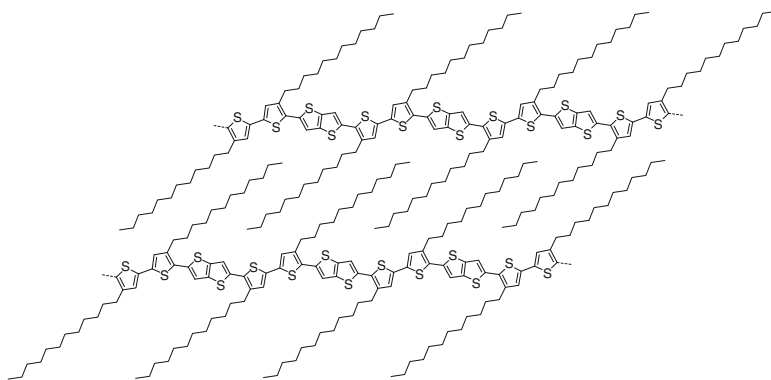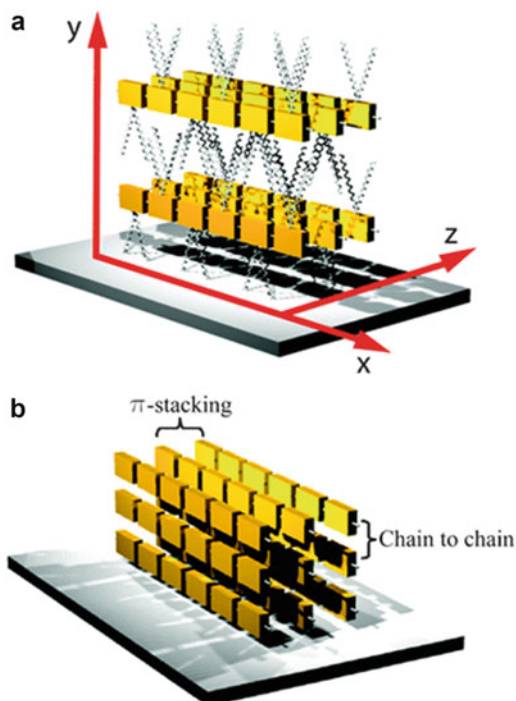

Fig. 9.4 Schematic of the packing of polymer chains of a saniditic liquid crystal with uniform side chain interdigitation

[18, 19]. The OFET performance improves on annealing above the mesophase transition temperature. Polymer **1** has no corresponding mechanism capable of improving the degree of order.

Figure 9.5 shows how the order of a saniditic liquid crystal polymer **3** changes with annealing. The top and middle three images show grazing incidence X-ray diffraction patterns and AFM images of the surfaces, respectively. The left-hand
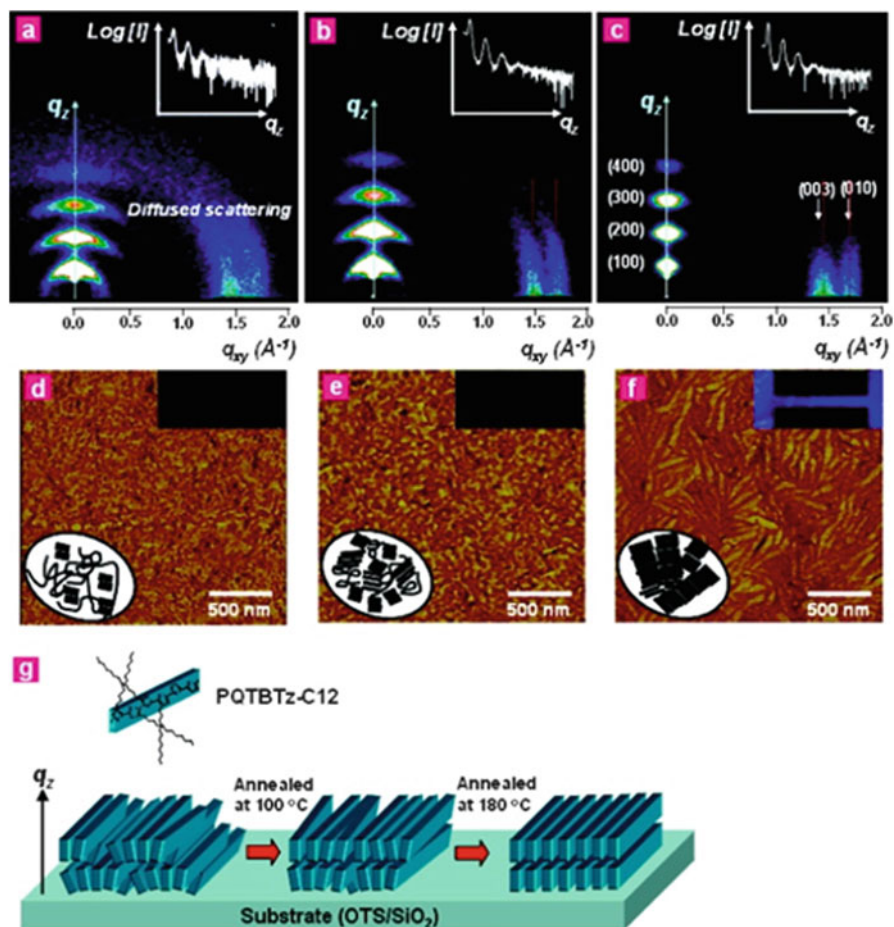
Fig. 9.5 Effects of thermal annealing on molecular orientation and morphological features of the saniditic liquid crystal 3. 2D grazing incidence X-ray diffraction patterns of the thin films spin-coated onto OTS-treated SiO₂ substrates for various annealing temperatures: (**a**) as-spun, (**b**) 100°C, (**c**) 180°C. The data are plotted versus the scattering vector q. (The *insets* in (**a**), (**b**), and (**c**) show the log-scale X-ray intensity profiles along the q_z axis, and the crystallographic assignments of the peaks are labelled.) AFM topographs of the thin films spin-coated onto the OTS-treated SiO₂ substrates for various annealing temperatures: (**d**) as-spun, (**e**) 100°C, (**f**) 180°C. The insets in (**d**), (**e**), and (**f**) show the polarized optical microscope images (*right-up*) and schematic features of self-organization of the polymer chains for various annealing temperatures (*left-down*). (**g**) Schematic representation of liquid-crystalline domains in thin films for various annealing temperatures, where q_z is the surface normal direction (Reprinted with permission from [17]. Copyright (2009) American Chemical Society)

images are taken from spin-cast films whilst the middle and right hand images correspond to films annealed at 100°C and 180°C, respectively, the former below the mesophase transition temperature. The bottom set of cartoons illustrate improved

crystallisation on annealing. On annealing to the mesophase, the backbones can freely move and reorganise into a more-ordered state, whilst removing defects. Upon cooling, the side chains recrystallise to capture and maintain the high level of layer order. The (h00) set of spots in the X-ray images correspond to lamellar stacking due to the alkyl side-chains with a d spacing of 21 Å. The X-ray patterns in Fig. 9.5 provide evidence of improved order following annealing in the mesophase; in particular the narrow spots in the out-of-plane, q_z, direction showing perfect edge-on orientation. The corresponding AFM image, Figure 9.5, shows polycrystalline structures with rod-shape grains, which arise from the self-organization of the perpendicularly oriented polymer chains. Annealing in the mesophase improved the FET mobility of **3** by an order of magnitude.

9.3.2 *Oriented OFETs Using Liquid Crystalline Semiconductors*

As discussed in detail in Chaps. 2 and 5, electronic transport in organic semiconductors occurs by hopping between sites, which may be traps, single molecules, several repeat units of a polymer chain or even a number of delocalised chain segments in high-mobility conjugated mainchain polymers [20]. For highly conjugated polymers and extended oligomers, the hopping may be intramolecular, between different sites on the same chain or intermolecular between sites on neighbouring chains. The charge transport is anisotropic since the rates of intramolecular and intermolecular hopping are not equal. The first application of liquid crystals to OFETs exploited the anisotropic carrier transport properties of the liquid crystalline polyfluorene copolymer **4** when uniformly oriented [21]. The polymer **4** exhibits a nematic phase above 265°C, as shown in Table 9.1. A top-gate, bottom-drain device configuration was used. The source and drain electrodes were deposited onto a rubbed polyimide alignment layer. The copolymer was then deposited and annealed in the liquid crystalline phase. The nematic ordering was maintained in a glassy state by rapid quenching to prevent recrystallisation and the dielectric layer and gate electrode were then sequentially deposited. The FET mobility was 2×10^{-2} cm^2 V^{-1} s^{-1} when the quenched glass was oriented along the transport direction between the source and drain. The mobility was an order of magnitude less for perpendicular orientation. This result shows that the rate of intra-chain transport of holes is very much greater than the hopping rate between chains and aligning the chains along the channel minimises the number of inter-chain hops. Similar results were found for a uniformly oriented oligofluorene and polyfluorene [22].

The lamellar liquid crystalline polymer **2** has a high-temperature phase transition at about 251°C. Heating above this phase transition produces films with a smectic-like, chain-extended conformation in which the polymer chains assemble into crystalline nano-ribbons with a characteristic width of 70–80 nm, consistent with the length of the fully extended polymer chain backbone. These ribbons, separated by grain boundaries, extend over several micrometers in the direction of π−π stacking

Fig. 9.6 SEM image of a uniaxially aligned thin film of 2 produced by zone casting. The scale denotes a length of 200 nm. The extended polymer chains are aligned in the *horizontal directions* with smectic-like organisation (Reproduced with pernmission from [24] Copyright @ 2011 WILEY-VCH)
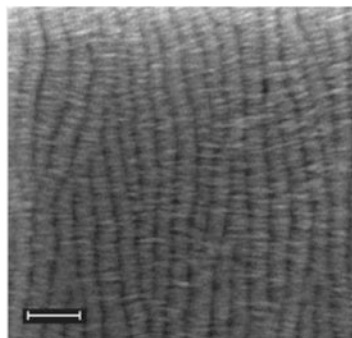
[23]. A zone casting method, followed by annealing at 275°C, was used to uniaxially align the nano-ribbons, producing films with structures shown in Fig. 9.6 [24]. This involved dispensing a solution of the polymer through a linear-shaped nozzle onto a linearly translating substrate, whose speed was carefully controlled, as was the rate at which the solution was dispensed by the plunger. The temperatures of the substrate and the solution were also optimised to control the drying speed, in order to prevent nucleation in solution and to induce uniaxial alignment of the polymer near the drying front.

The mobility of the aligned polymer was anisotropic having a value of 0.13 cm^2 V^{-1} s^{-1} parallel to the polymer chains, and a factor of five less in the perpendicular orientation. The mobility along the chain direction does not reflect directly the fast, intrachain, charge transport along the polymer backbone, but is limited by disordered grain boundaries between the chain-extended ribbons occurring on a 60–80 nm length scale. Along the ribbons, a close inspection of Fig. 9.6 shows that domain boundaries are also encountered on a 20–30 nm length scale. In these grain boundaries charges encounter a relatively favourable parallel chain orientation. The measured mobility anisotropy of about 5 is close to the ratio of grain sizes encountered in the two transport directions.

9.3.3 Polymer Light-Emitting Field Effect Transistors

Polymers, such as **4**, with a nematic phase generally exhibit mobility mobility values typically at least an order of magnitude less than that of the saniditic materials discussed in Sect. 9.3.1. However, as discussed in more detail in Chaps. 2 and 5, the former class of materials are often efficient light-emitters and, as such, they are promising candidates for ambipolar, light-emitting, field-effect transistors (LEFETs). These devices can form electron and hole accumulation layers simultaneously within the channel between the source and drain electrodes, as illustrated in Fig. 9.7. Charge recombination occurs at the interface between the two regions and thus light emission is observed. LEFETs are currently the subject
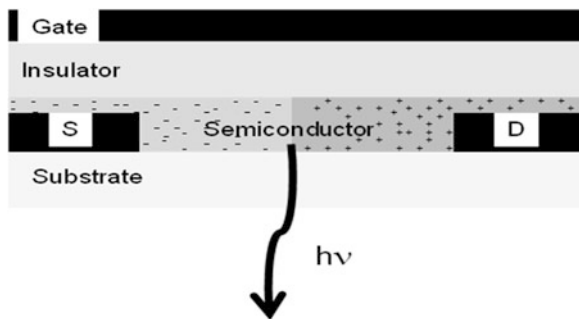
Fig. 9.7 Schematic of the structure of a top gate LEFET. Under appropriate driving conditions, the source and drain electrodes inject charge carriers of different sign so that both electrons and holes accumulate in the channel. Carrier recombination and light emission occurs at the intersection between the accumulation regions (Reproduced with pernmission from [29] Copyright @ 2011 WILEY-VCH)

of a lot of interest because they are compatible with waveguide transmission of the emitted light for optoelectronic integrated circuits. High current densities can be obtained, which generate an attractive architecture for the potential realization of electrically-pumped organic lasers. The liquid crystalline poly(9,9-dioctylfluorene-*alt*-benzothiadiazole) **5** (F8BT), possesses HOMO and LUMO energies with similar barriers for electron- and hole-injection from gold electrodes and so has been widely used in LEFETs [25–27]. In most cases the transistors' characteristics are optimised following annealing from the liquid crystaline phase, although the resulting film is polycrystalline at room temperature [27]. However, high-temperature annealing results in high surface roughness, which increases the losses of the optical wave-guide. Modification of the gold electrodes with a 1-decanethiol, self-assembled monolayer (SAM) significantly improves performance of the low-temperature (120°C) devices, allowing efficient charge injection into F8BT films deposited on top [25]. The emitted light from a LEFET based on polymer **5** was coupled efficiently into the resonant mode of a passive Ta_2O_5 waveguide by placing the recombination zone of the LEFET directly above the waveguide ridge [28]. The waveguide provides distributed feedback by means of a grating and optically pumped lasing is obtained. Interestingly, low temperature annealing was used to give an amorphous, rather than a polycrystalline, film and so minimise light scattering. A LEFET was constructed with polymer **5** uniaxially-aligned in a monodomain [26]. The location of the emission along the channel between the source and drain is dependent on the applied voltage between them. The width of the emission zone is 5–10 times greater than that when the polymer is aligned parallel to the current than for perpendicular alignment, implying a more than 100 times smaller recombination rate constant than expected for Langevin recombination. This result suggests that anisotropic mobility affects the probability of exciton formation, decreasing it parallel to the aligned chains and increasing it in the perpendicular direction.

9.4   Columnar Liquid Crystals in OFETs

Discotic liquid crystals are oriented in columns separated by molten aliphatic chains and consequently they can conduct charge efficiently along the columns in one dimension. The organization of the different phases is described in Chaps. 1 and 2 as well as elsewhere [30, 31] and the efficiency of charge transport can be directly related to the short intermolecular spacing and order of different types of mesophase, as discussed in detail in Chaps. 2 and 3. Some mesomorphic derivatives of hexabenzocoronene, possess values of hole mobility above $0.2\,\mathrm{cm^2\,V^{-1}\,s^{-1}}$ in the discotic phase at room temperature, while others exhibit values above $1\,\mathrm{cm^2\,V^{-1}\,s^{-1}}$ in a crystalline phase at elevated temperatures [32]. However, these measurements give the value of the local mobility only and the reported value of the charge mobility is much lower ($\leq 0.02\,\mathrm{cm^2\,V^{-1}\,s^{-1}}$) in actual OFET devices [33, 34]. This behaviour is mainly due to the presence of poor contacts as well as the difficulty in obtaining uniform macroscopic alignment and in optimising order in solution-processed devices. In-plane transport is required between the source and drain electrodes of OFETS, so that the columns must have an edge-on, or homogeneous configuration, as illustrated in Fig. 9.8. Zone casting was used to provide a homogeneously aligned film of the hexabenzocoronene **6**, whose structure is shown in Table 9.2, giving one of the best performing discotic columnar OFET devices with
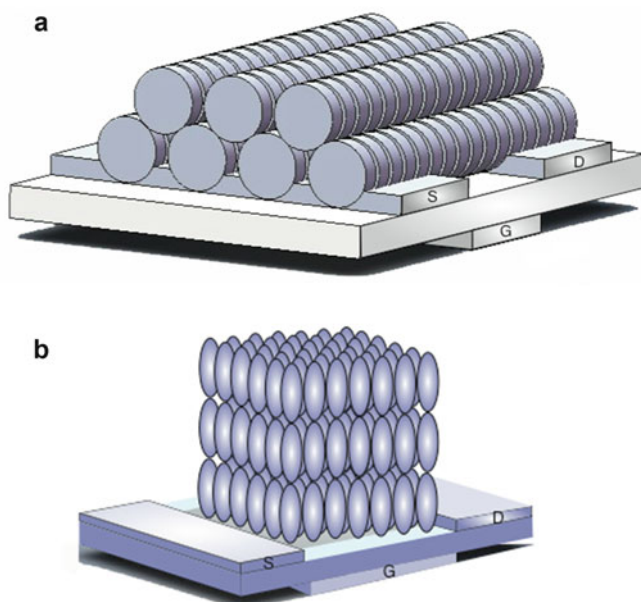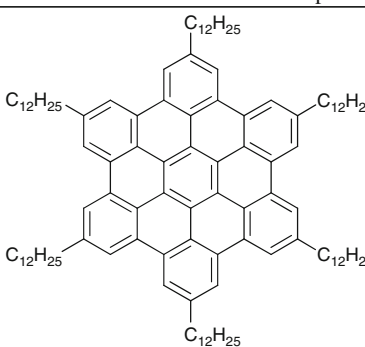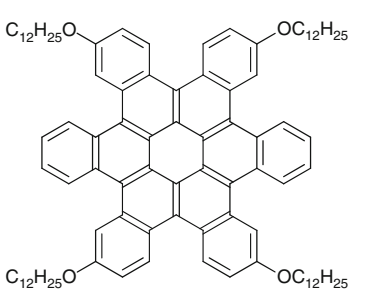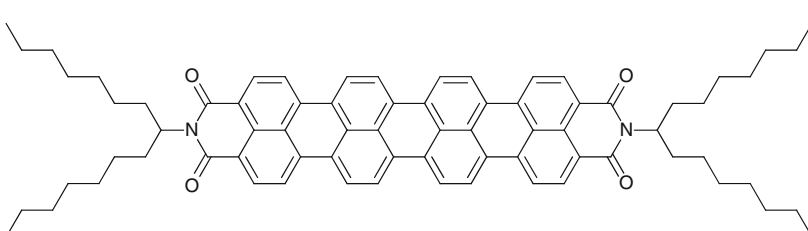

Fig. 9.8 Schematic illustration of optimum orientation of (**a**) columnar and (**b**) smectic liquid crystals for OFET operation (Reproduced with pernmission from [29] Copyright @ 2011 WILEY-VCH)

Table 9.2 Chemical structures of compounds with columnar phases

6

HBC-C$_{12}$: Tg-Col$_1$ = 42°C; Col$_1$- I = 107°C

7

HBC-C$_{O12}$: Cr-Col$_1$ = 91°C; Col$_1$- I = 285°C

8

SWQDI: Col$_p$- Col$_{ho}$ = 188°C; Col$_{ho}$- I > 500°C
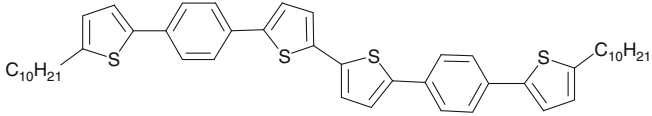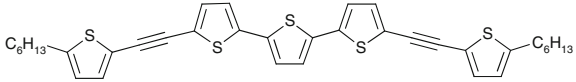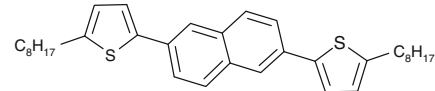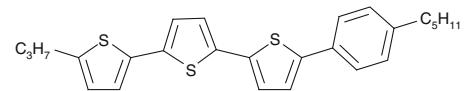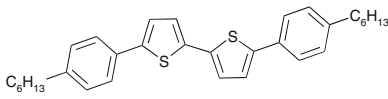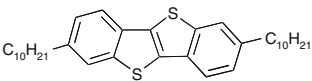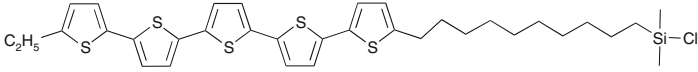
a hole mobility of 0.01 cm^2 V^{-1} s^{-1} [33, 35]. Electron and X-ray diffraction confirm that the zone-cast layer is crystalline with an edge-on orientation to the substrate. Vertically adjacent layers are tilted at ±45° to the substrate with a herringbone arrangement. The discotic hexabenzocoronene **7** has a non-planar core, which arises as a result of steric congestion attributable to its peripheral phenyl groups [34]. Homogeneous alignment was realised by spin-casting the material onto a SAM-modified SiO$_2$ insulator and OFETs with a mobility of 0.02 cm^2 V^{-1} s^{-1}were obtained. It is suggested that non-planarity may improve the mobility, because the π-surfaces of contorted molecules can approach each other and arrange themselves in very different ways. Ambipolar, organic field-effect transistors (OFETs) are of

special interest owing to their application in complementary-like circuits or light-emitting field-effect transistors. Swallow-tailed, quarterrylene-tetracarboxdiimide (SWQDI) compounds with discotic columnar superstructures, see **8**, were utilised as an active layer in ambipolar thin film transistors [36]. The work function of gold lies approximately in the middle of the band-gap of **8**. An OFET with a drop-cast active layer has a roughly equal magnitude of electron and hole mobility of $\approx 1 \times 10^{-3}$ cm^2 V^{-1} s^{-1}. Interestingly, hole transport disappears and electron mobility is reduced on annealing to a more ordered film.

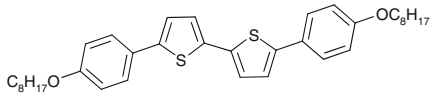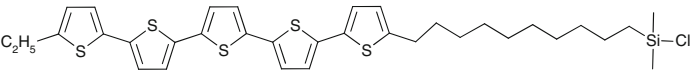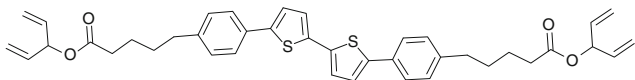## 9.5 Low-Mass Smectic Liquid Crystals in OFETs

Low-molar-mass, smectic liquid crystals self-organise in layers with order in two dimensions. Silane-based surfactants are generally used to give the homeotropic alignment required to provide in-plane transport between the electrodes of OFETs, see Fig. 9.8. There are a number of smectic phases as illustrated in Chaps. 1 and 2 as well as elsewhere [30, 31]. In the smectic A and C phases the packing in the layers is fluid-like, while the more-ordered, crystalline smectics, with hexatic, hexagonal or herring-bone packing, facilitate greater π-π overlap, as discussed in more detail in Chaps. 1 and 2 as well as elsewhere. Many smectic liquid crystals show ambipolar transport [37]. Some high-performance, thin-film transistors with a mobility of up to 0.4 cm^2 V^{-1} s^{-1} have active layers of thermally-evaporated thiophene-phenylene oligomers, for example compound **9**, whose chemical structure is shown in Table 9.3, with smectic phases at high temperatures [38]. However, the liquid crystalline properties are not directly utilised in devices. Crystal grain boundaries can be avoided by annealing and reorganization in the fluid smectic phase, followed by slow cooling through more-ordered smectic phases by the process of paramorphosis [39, 40]. Hence, a monodomain crystalline sample of compound **10** was prepared by solution processing and annealing on a rubbed polyimide layer, as shown in Fig. 9.9. This contrasts with the leaf-like multi-domain crystals that are produced by spin-casting onto an untreated substrate. An OFET mobility of 0.02 cm^2 V^{-1} s^{-1} was obtained for the monodomain sample, which is an order of magnitude larger than that found using multi-domain samples of the same material [39]. The mobility is anisotropic, possibly because the tilting of the molecules in the layers reduces the π-π overlap in one direction. Paramorphosis does not occur, if the crystalline phase has a significantly different molecular arrangement to that of the mesophases. Interestingly, a thiophene-naphthalene-based mesogen, compound **11**, retains its layered structure in a polycrystalline phase at room temperature in a thermally deposited OFET, giving a high carrier mobility of 0.14 cm^2 V^{-1} s^{-1} [41]. However, its mobility decreases following annealing in the smectic phase at 100°C, possibly because of cracking of the organic layer caused by differential degrees of expansion of the layer and the substrate. A mesogen **12**, with a room temperature smectic phase, showed a time-of-flight carrier mobility of 0.07 and 0.2 cm^2 V^{-1} s^{-1} for holes and electrons respectively [42]. A solution-processed

Table 9.3 Chemical structures of compounds with smectic phases

9

Dec-(TPhT)$_2$-Dec: Cr-SmX = 316°C; SmX-I = 351°C

Dec-(TPhT)$_2$-Dec: Cr-SmX = 316°C; SmX-I = 351°C

10

Cr-SmC = 92°C; SmC-SmA = 111°C; SmA-N = 115°C; N-I = 180°C

11

8-TNAT-8: Cr-SmX = 95°C; SmX-I = 182°C

12

Cr-SmX < −50°C; SmX–I = 57°C

13

DH-PTTP: Cr-SmC 232°C; SmF-SmB 139°C; SmB-SmC = 150°C; SmC-SmA = 235°C; SmA-I = 239°C

14

C$_{10}$-BTBT: Cr-SmC 232°C; SmF-SmB 139°C; SmB-SmC = 150°C; SmC-SmA = 235°C; SmA-I = 239°C

15

8-TTP-8: Cr-SmC 232°C; SmG-SmF 139°C; SmF-SmC = 150°C; SmC-I = 235°C

Table 9.3 (continued)

16

Doo-P2TP

17

18

Cr-SmG = 75°C; SmG-I = 174°C
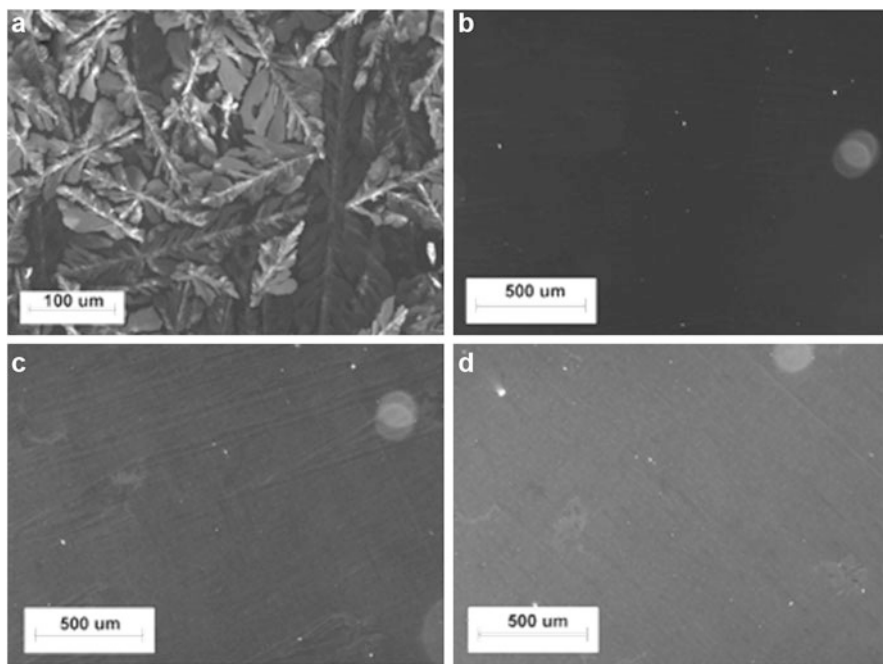
Fig. 9.9 Light transmission micrographs of two films of compound **10** (polarizer in the *horizontal*, analyzer in the *vertical* direction): (**a**) untreated, as-spun film; (**b**) monodomain with the rubbing direction of the PI layer parallel to the analyzer; (**c**) rubbing direction at 22.5° with respect to the analyzer; (**d**) rubbing direction at an angle of 45° with respect to the analyzer (Reprinted with permission from [39]. Copyright (2006) American Chemical Society)

film of compound **12** exhibited hole mobility values of up to 0.04 cm^2 V^{-1} s^{-1} in an OFET, when well aligned by a silane-based, self-assembled monolayer after annealing [43, 44]. A similar result was obtained on a 3 % strained polyimide substrate, which demonstrates the suitabilty of smectic compounds for flexible plastic electronics [45]. Bottom-contact OFETs with a mobility value of up to 0.03 cm^2 V^{-1} s^{-1} have been fabricated using a very simple process involving neither solvents nor vacuum-deposition. A liquid-crystalline organic semiconductor, **13**, was melted directly onto a SiO$_2$ dielectric layer treated with a surfactant to promote homeotropic alignment. A surfactant-treated cover-slide was placed on top of the powder before melting to prevent dewetting. The melting and cooling conditions were optimised to maximise charge mobility, which was significantly larger than that obtained for thermally evaporated films.

Recently some solution processed smectic materials have shown extremely high values of OFET mobility. Compound **14** has a benzothienobenzothiophene core and exhibits a smectic A (SmA) phase in the temperature range from 95 to 122°C. It has a mobility up to 0.86 cm^2 V^{-1} s^{-1} when spin-coated at room temperature and annealed at 80°C. Similarly processed compounds with the same backbone but with alkyl chains of different lengths showed mobilities as high as 2.75 cm^2 V^{-1} s^{-1} [46], the mobility tending to increase with alkyl chain length. The extremely high mobility is attributed to excellent molecular overlap resulting from the herringbone monoclinic crystal structure, which enhances the sulfur–sulfur interaction, and the hydrophobic interactions effected by long alkyl chains [47]. For films deposited by solution processing at room temperature, recrystallization takes place on the substrate during solvent evaporation and the inhomogeneity of the films is not fully improved by post-thermal annealing. The wetting and homogeneity of thin films of **14** was substantially improved by spin-coating when in the liquid crystalline phase, resulting in extremely high mobilities up to 3 cm^2 V^{-1} s^{-1} [48]. Similarly the mobility of the terthiophene oligomer **15** increased by over an order of magnitude to 0.1 cm^2 V^{-1} s^{-1} by spin-casting in the smectic phase [48].

Photoalignment has been used to homogeneously align the phenylene-thiophene compound **16**, which possesses a high-temperature smectic phase [49, 50]. The magnitude of the mobility was enhanced, when the direction of electronic transport was parallel to the direction of the intermolecular hops (perpendicular to the molecular rods) [49]. An OFET hole mobility of 0.05 cm^2 V^{-1} s^{-1} was obtained, compared to a value of 0.003 cm^2 V^{-1} s^{-1} measured in the orthogonal direction. This is the opposite result to that obtained for the mainchain polymer, discussed in Sect. 9.3.2 above. The result for **16** is not surprising since intramolecular hopping, which is faster than intermolecular hopping in polymers, is a meaningless concept for so short a molecular core and intermolecular transport is faster within a smectic layer rather than between layers.

Self-assembled monolayer FETs (SAMFETs), where the semiconductor is a monolayer spontaneously formed by self-assembly on the dielectric layer, is a promising technology for the mass production of organic electronics. However, the

presence of defects limit charge transport, so that devices with channels of only sub-micron length work well. SAMFETs with long-range intermolecular π-π coupling in the monolayer were obtained by dense packing with liquid-crystalline compounds, for example compound **17** [51]. These materials consist of a π-conjugated mesogenic core separated by a long aliphatic chain from a monofunctionalised anchor group. The resulting SAMFETs exhibit a bulk-like carrier mobility up to $0.04 \ cm^2 \ V^{-1} \ s^{-1}$, large current modulation and high reproducibility.

OFETs require organic semiconductors with a high glass transition temperature for long-term stability. An alternative way to ensure stability makes use of the *in-situ* crosslinking of a thin film of reactive mesogens, which are low-molar-mass liquid crystals with at least two polymerisable groups often separated from the molecular core of the liquid crystal by flexible aliphatic spacer units [52–56]. Reactive mesogens often exhibit a low viscosity and can be designed to exhibit mesophases at low temperatures, so they can be easily ordered or macroscopically aligned in thin films at or near room temperature. The order is then permanently fixed by cross-linking of adjacent molecules either by irradiation with ultraviolet light or thermal polymerisation. The use of reactive mesogens in OLEDs and photovoltaics is discussed in Chaps. 7 and 8, respectively. Chapter 5 discusses charge transport in these materials. Compound **18** is an example of a photopolymerisable smectic liquid crystal with non-conjugated diene polymerisable terminal groups decoupled by aliphatic chains from the semiconducting aromatic core. Thermal or photopolymerisation links the reactive groups together. In this case each molecule has two reactive groups so a highly crosslinked, insoluble and intractable polymer network of mesogenic units is obtained. Different types of polymerisable groups, such as methacrylate, acrylate, diene and oxetane reactive groups, have been used. Scheme 9.1 shows the general structures of the polymer backbones formed on crosslinking. Photopolymerisation offers the further possibility of pixellation by photolithography. Unexposed and, therefore, non-crosslinked, regions are still soluble in organic solvents and are simply removed by washing in the original spin-casting solvent. OFETs fabricated from both crosslinked and uncrosslinked films of smectic reactive mesogens with reactive end-groups, such as **18**, have been studied [57–59]. Relatively low values of mobility are found, $<0.005 \ cm^2 \ V^{-1} \ s^{-1}$, possibly because of disorder induced by the long terminal aliphatic chains. On crosslinking the mobility decreases for most of the compounds studied by at least a factor of five, possibly because the layer structure of the smectic mesogens is disrupted, when the end groups of the molecules form a covalently bonded polymer backbone. However, this result may not be general as time-of-flight mobility values, $>10^{-2} \ cm^2 \ V^{-1} \ s^{-1}$, were found to be similar for smectic reactive mesogens with oxetane reactive end-groups before and after polymerisation [60]. Crosslinking was also shown not to degrade charge transport in an OFET based on star-shaped molecules and in a nematic reactive mesogen with diene photoreactive endgroups studied with time-of-flight measurements [61, 62].

Scheme 9.1 Polymerisable groups, acryalte, methacrylate, diene and oxetane groups from top to bottom, and the corresponding polymer backbones formed on polymerisation of these monomers
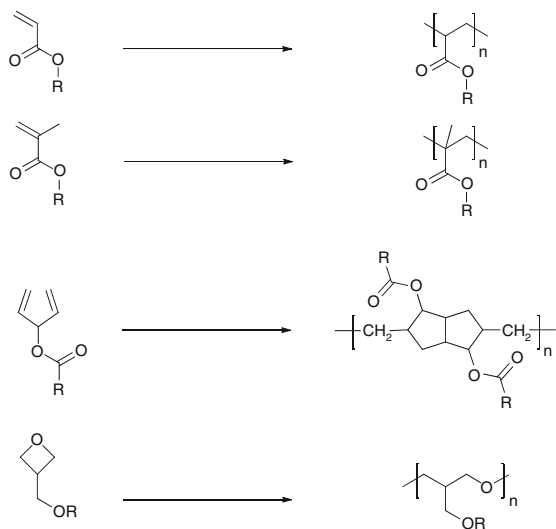
9.6 Conclusions

There have been many major advances in liquid crystalline organic semiconductors in recent years including the ability of saniditic liquid crystals to allow very high values of the charge carrier mobility in polymer-based OFETs with state-of-the art performance [63]. The high values of the mobility results from re-ordering of both the aliphatic layers and the conjugated polymer backbone into close-packed structures. The side-chains can interdigitate between vertically adjacent lamellae and facilitate thereby the formation of large domains with a high degree of molecular order. The use of more-disordered, liquid-crystalline, semiconducting polymers in LEFETs is a promising development, although more investigation is needed on why recombination is inhibited in aligned samples. Although the time-of-flight charge carrier mobility of columnar and smectic materials can have very high values, $>0.1 \, \text{cm}^2 \, \text{V}^{-1} \, \text{s}^{-1}$, the OFET mobility values are mostly significantly lower particularly in solution-processed devices. This is a critical issue, since solution processing is compatible with high-volume, large-scale manufacturing. An exception is the recent work from the Hiroshima and Hanna groups who obtained state-of-the-art mobilities $>1 \, \text{cm}^2 \, \text{V}^{-1} \, \text{s}^{-1}$ from materials having the benzothienobenzothiophene core and high temperature smectic phases. The mobility and film quality improved by spin-casting in the smectic phase. Thus, sample processing has emerged as a critical factor, which influences electronic and optoelectronic device properties. Zone and drop casting are alternative solution-based methods to produce highly ordered thin films. An extremely high FET mobility was obtained from a dip-cast sample of a semiconducting polymer, which is not liquid crystalline, following annealing [64]. A similar approach would allow the anisotropic properties of liquid crystalline polymers to be best exploited. Although initial efforts to obtain monodomain OFETs

are promising, more work is needed to further exploit this important capability of liquid crystals, especially as defects are known to limit charge transport in devices. Very often the liquid crystalline phases of mesomorphic organic semiconductors exist at high temperatures and annealing at these temperatures may well not be compatible with efficient and cost-effective manufacturing processes. Alternatively, solvent vapour annealing may be carried out at lower temperatures using solvents with high boiling points as plasticisers [65].

In conclusion, the application of self-organised materials to organic electronics is maturing well. Some liquid crystalline organic semiconductors are used in devices with state-of-the-art performance, whilst others, though not optimized, give novel device properties or alternative processing opportunities. As the research fields of organic electronics become more sophisticated, more complex devices will be required, so that the ability to pattern and fix self-assembled, liquid-crystalline organic semiconductors will be become increasingly important.

References

1. Coropceanu, V., Cornil, J., da Silva Filho, D.A., Olivier, Y., Silbey, R., Brédas, J.L.: Charge transport in organic semiconductors. Chem. Rev. **107**(4), 926–952 (2007)
2. Sirringhaus, H.: Device physics of solution-processed organic field-effect transistors. Adv. Mater. **17**(20), 2411–2425 (2005). doi:10.1002/adma.200501152
3. Zaumseil, J., Sirringhaus, H.: Electron and ambipolar transport in organic field-effect transistors. Chem. Rev. **107**(4), 1296–1323 (2007)
4. Allard, S., Forster, M., Souharce, B., Thiem, H., Scherf, U.: Organic semiconductors for solution-processable field-effect transistors (OFETs). Angew. Chem. Int. Ed. **47**(22), 4070–4098 (2008)
5. Newman, C.R., Frisbie, C.D., da Silva, D.A., Bredas, J.L., Ewbank, P.C., Mann, K.R.: Introduction to organic thin film transistors and design of n-channel organic semiconductors. Chem. Mater. **16**(23), 4436–4451 (2004). doi:10.1021/cm049391x
6. Sirringhaus, H., Brown, P.J., Friend, R.H., Nielsen, M.M., Bechgaard, K., Langeveld-Voss, B.M.W., Spiering, A.J.H., Janssen, R.A.J., Meijer, E.W., Herwig, P., De Leeuw, D.M.: Two-dimensional charge transport in self-organized, high-mobility conjugated polymers. Nature **401**(6754), 685–688 (1999)
7. Chang, J.F., Clark, J., Zhao, N., Sirringhaus, H., Breiby, D.W., Andreasen, J.W., Nielsen, M.M., Giles, M., Heeney, M., McCulloch, I.: Molecular-weight dependence of interchain polaron delocalization and exciton bandwidth in high-mobility conjugated polymers. Phys. Rev. B Conden. Matter Mater. Phys. **74**(11) (2006)
8. Kline, R.J., McGehee, M.D.: Morphology and charge transport in conjugated polymers. Polym. Rev. **46**(1), 27–45 (2006)
9. Kline, R.J., McGehee, M.D., Toney, M.F.: Highly oriented crystals at the buried interface in polythiophene thin-film transistors. Nat. Mater. **5**(3), 222–228 (2006)
10. Tsao, H.N., Mullen, K.: Improving polymer transistor performance via morphology control. Chem. Soc. Rev. **39**(7), 2372–2386 (2010)
11. Ong, B.S., Wu, Y., Liu, P., Gardner, S.: High-performance semiconducting polythiophenes for organic thin-film transistors. J. Am. Chem. Soc. **126**(11), 3378–3379 (2004)
12. McCulloch, I., Heeney, M., Bailey, C., Genevicius, K., MacDonald, I., Shkunov, M., Sparrowe, D., Tierney, S., Wagner, R., Zhang, W., Chabinyc, M.L., Kline, R.J., McGehee, M.D., Toney, M.F.: Liquid-crystalline semiconducting polymers with high charge-carrier mobility. Nat. Mater. **5**(4), 328–333 (2006)

13. McCulloch, I., Heeney, M., Chabinyc, M.L., Delongchamp, D., Kline, R.J., Cölle, M., Duffy, W., Fischer, D., Gundlach, D., Hamadani, B., Hamilton, R., Richter, L., Salleo, A., Shkunov, M., Sparrowe, D., Tierney, S., Zhang, W.: Semiconducting thienothiophene copolymers: design, synthesis, morphology, and performance in thin-film organic transistors. Adv. Mater. **21**(10–11), 1091–1109 (2009)

14. Heeney, M., Bailey, C., Genevicius, K., Shkunov, M., Sparrowe, D., Tierney, S., McCulloch, I.: Stable polythiophene semiconductors incorporating thieno[2,3-6]thiophene. J. Am. Chem. Soc. **127**(4), 1078–1079 (2005)

15. Hamadani, B.H., Gundlach, D.J., McCulloch, I., Heeney, M.: Undoped polythiophene field-effect transistors with mobility of 1 cm^2 V^{-1} s^{-1}. Appl. Phys. Lett. **91**(24), P243512 (2007)

16. Li, Y., Wu, Y., Liu, P., Birau, M., Pan, H., Ong, B.S.: Poly(2,5-bis(2-thienyl)-3,6-dialkylthieno[3,2-b]thiophene)s-high-mobility semiconductors for thin-film transistors. Adv. Mater. **18**(22), 3029–3032 (2006)

17. Kim, D.H., Lee, B.L., Moon, H., Kang, H.M., Jeong, E.J., Park, J.I., Han, K.M., Lee, S., Yoo, B.W., Koo, B.W., Kim, J.Y., Lee, W.H., Cho, K., Becerril, H.A., Bao, Z.: Liquid-crystalline semiconducting copolymers with intramolecular donor-acceptor building blocks for high-stability polymer transistors. J. Am. Chem. Soc. **131**(17), 6124–6132 (2009)

18. Delongchamp, D.M., Kline, R.J., Jung, Y., Lin, E.K., Fischer, D.A., Gundlach, D.J., Cotts, S.K., Moad, A.J., Richter, L.J., Toney, M.F., Heeney, M., McCulloch, I.: Molecular basis of mesophase ordering in a thiophene-based copolymer. Macromolecules **41**(15), 5709–5715 (2008)

19. DeLongchamp, D.M., Kline, R.J., Lin, E.K., Fischer, D.A., Richter, L.J., Lucas, L.A., Heeney, M., McCulloch, I., Northrup, J.E.: High carrier mobility polythiophene thin films: structure determination by experiment and theory. Adv. Mater. **19**(6), 833–837 (2007)

20. Chang, J.F., Sirringhaus, H., Giles, M., Heeney, M., McCulloch, I.: Relative importance of polaron activation and disorder on charge transport in high-mobility conjugated polymer field-effect transistors. Phys. Rev. B Conden. Matter Mater. Phys. **76**(20), 205204 (2007)

21. Sirringhaus, H., Wilson, R.J., Friend, R.H., Inbasekaran, M., Wu, W., Woo, E.P., Grell, M., Bradley, D.D.C.: Mobility enhancement in conjugated polymer field-effect transistors through chain alignment in a liquid-crystalline phase. Appl. Phys. Lett. **77**(3), 406–408 (2000)

22. Yasuda, T., Fujita, K., Tsutsui, T., Geng, Y., Culligan, S.W., Chen, S.H.: Carrier transport properties of monodisperse glassy-nematic oligofluorenes in organic field-effect transistors. Chem. Mater. **17**(2), 264–268 (2005)

23. Delongchamp, D.M., Kline, R.J., Jung, Y., Germack, D.S., Lin, E.K., Moad, A.J., Richter, L.J., Toney, M.F., Heeney, M., McCulloch, I.: Controlling the orientation of terraced nanoscale "ribbons" of a poly(thiophene) semiconductor. ACS Nano **3**(4), 780–787 (2009)

24. Lee, M.J., Gupta, D., Zhao, N., Heeney, M., McCulloch, I., Sirringhaus, H.: Anisotropy of charge transport in a uniaxially aligned and chain-extended, high-mobility, conjugated polymer semiconductor. Adv. Funct. Mater. **21**(5), 932–940 (2011)

25. Gwinner, M.C., Khodabakhsh, S., Giessen, H., Sirringhaus, H.: Simultaneous optimization of light gain and charge transport in ambipolar light-emitting polymer field-effect transistors. Chem. Mater. **21**(19), 4425–4433 (2009)

26. Zaumseil, J., Groves, C., Winfield, J.M., Greenham, N.C., Sirringhaus, H.: Electron-hole recombination in uniaxially aligned semiconducting polymers. Adv. Funct. Mater. **18**(22), 3630–3637 (2008)

27. Zaumseil, J., Donley, C.L., Kim, J.S., Friend, R.H., Sirringhaus, H.: Efficient top-gate, ambipolar, light-emitting field-effect transistors based on a green-light-emitting polyfluorene. Adv. Mater. **18**(20), 2708–2712 (2006)

28. Gwinner, M.C., Khodabakhsh, S., Song, M.H., Schweizer, H., Giessen, H., Sirringhaus, H.: Integration of a rib waveguide distributed feedback structure into a light-emitting polymer field-effect transistor. Adv. Funct. Mater. **19**(9), 1360–1370 (2009)

29. O'Neill, M., Kelly, S.M.: Ordered materials for organic electronics and photonics. Adv. Mater. **23**(5), 566–584 (2011)

30. Funahashi, M.: Development of liquid-crystalline semiconductors with high carrier mobilities and their application to thin-film transistors. Polym. J. **41**(6), 459–469 (2009)

31. Pisula, W., Zorn, M., Chang, J.Y., Mullen, K., Zentel, R.: Liquid crystalline ordering and charge transport in semiconducting materials. Macromol. Rapid Commun. **30**(14), 1179–1202 (2009)

32. Van De Craats, A.M., Warman, J.M., Fechtenkötter, A., Brand, J.D., Harbison, M.A., Müllen, K.: Record charge carrier mobility in a room-temperature discotic liquid-crystalline derivative of hexabenzocoronene. Adv. Mater. **11**(17), 1469–1472 (1999)

33. Pisula, W., Menon, A., Stepputat, M., Lieberwirth, I., Kolb, U., Tracz, A., Sirringhaus, H., Pakula, T., Müllen, K.: A zone-casting technique for device fabrication of field-effect transistors based on discotic hexa-perihexabenzocoronene. Adv. Mater. **17**(6), 684–688 (2005)

34. Xiao, S., Myers, M., Miao, Q., Sanaur, S., Pang, K., Steigerwald, M.L., Nuckolls, C.: Molecular wires from contorted aromatic compounds. Angew. Chem. Int. Ed. **44**(45), 7390–7394 (2005)

35. Tracz, A., Jeszka, J.K., Watson, M.D., Pisula, W., Mullen, K., Pakula, T.: Uniaxial alignment of the columnar super-structure of a hexa (alkyl) hexa-peri-hexabenzocoronene on untreated glass by simple solution processing. J. Am. Chem. Soc. **125**(7), 1682–1683 (2003)

36. Tsao, H.N., Pisula, W., Liu, Z., Osikowicz, W., Salaneck, W.R., Müllen, K.: From ambi- To unipolar behavior in discotic dye field-effect transistors. Adv. Mater. **20**(14), 2715–2719 (2008)

37. Iino, H., Hanna, J.: Ambipolar charge carrier transport in liquid crystals. Opto-Electron. Rev. **13**(4), 295–302 (2005)

38. Ponomarenko, S.A., Kirchmeyer, S., Elschner, A., Alpatova, N.M., Halik, M., Klauk, H., Zschieschang, U., Schmid, G.: Decyl-end-capped thiophene-phenylene oligomers as organic semiconducting materials with improved oxidation stability. Chem. Mater. **18**(2), 579–586 (2006)

39. Van Breemen, A.J.J.M., Herwig, P.T., Chlon, C.H.T., Sweelssen, J., Schoo, H.F.M., Setayesh, S., Hardeman, W.M., Martin, C.A., De Leeuw, D.M., Valeton, J.J.P., Bastiaansen, C.W.M., Broer, D.J., Popa-Merticaru, A.R., Meskers, S.C.J.: Large area liquid crystal monodomain field-effect transistors. J. Am. Chem. Soc. **128**(7), 2336–2345 (2006)

40. Vlachos, P., Mansoor, B., Aldred, M.P., O'Neill, M., Kelly, S.M.: Charge-transport in crystalline organic semiconductors with liquid crystalline order. Chem. Commun. **23**, 2921–2923 (2005)

41. Oikawa, K., Monobe, H., Nakayama, K.I., Kimoto, T., Tsuchiya, K., Heinrich, B., Guillon, D., Shimizu, Y., Yokoyama, M.: High carrier mobility of organic field-effect transistors with a thiophene-naphthalene mesomorphic semiconductor. Adv. Mater. **19**(14), 1864–1868 (2007)

42. Funahashi, M., Zhang, F., Tamaoki, N.: High ambipolar mobility in a highly ordered smectic phase of a dialkylphenylterthiophene derivative that can be applied to solution-processed organic field-effect transistors. Adv. Mater. **19**(3), 353–358 (2007)

43. Zhang, F., Funahashi, M., Tamaoki, N.: High-performance thin film transistors from semiconducting liquid crystalline phases by solution processes. Appl. Phys. Lett. **91**(6), 063515 (2007)

44. Zhang, F., Funahashi, M., Tamaoki, N.: Thin-film transistors based on liquid-crystalline tetrafluorophenylter thiophene derivatives: thin-film structure and carrier transport. Org. Electron. Phys. Mater. Appl. **10**(1), 73–84 (2009)

45. Liu, J., Zhang, R., Osaka, I., Mishra, S., Javier, A.E., Smilgies, D.-M., Kowalewski, T., McCullough, R.D.: Transistor paint: environmentally stable N-alkyldithienopyrrole and bithiazole-based copolymer thin-film transistors show reproducible high mobilities without annealing. Adv. Funct. Mater. **19**(21), 3427–3434 (2009)

46. Ebata, H., Izawa, T., Miyazaki, E., Takimiya, K., Ikeda, M., Kuwabara, H., Yui, T.: Highly soluble [1]benzothieno[3,2-b]benzothiophene (BTBT) derivatives for high-performance, solution-processed organic field-effect transistors. J. Am. Chem. Soc. **129**(51), 15732–15733 (2007)

47. Izawa, T., Miyazaki, E., Takimiya, K.: Molecular ordering of high-performance soluble molecular semiconductors and re-evaluation of their field-effect transistor characteristics. Adv. Mater. **20**(18), 3388–3392 (2008)

48. Iino, H., Hanna, J.I.: Availability of liquid crystallinity in solution processing for polycrystalline thin films. Adv. Mater. **23**(15), 1748–1751 (2011)

49. Fujiwara, T., Locklin, J., Bao, Z.: Solution deposited liquid crystalline semiconductors on a photoalignment layer for organic thin-film transistors. Appl. Phys. Lett. **90**(23), 232108 (2007)
50. O'Neill, M., Kelly, S.M.: Photoinduced surface alignment for liquid crystal displays. J. Phys. D: Appl. Phys. **33**(10), R67–R84 (2000)
51. Smits, E.C.P., Mathijssen, S.G.J., Van Hal, P.A., Setayesh, S., Geuns, T.C.T., Mutsaers, K.A.H.A., Cantatore, E., Wondergem, H.J., Werzer, O., Resel, R., Kemerink, M., Kirchmeyer, S., Muzafarov, A.M., Ponomarenko, S.A., De Boer, B., Blom, P.W.M., De Leeuw, D.M.: Bottom-up organic integrated circuits. Nature **455**(7215), 956–959 (2008)
52. Hikmet, R.A.M., Lub, J.: Anisotropic networks and gels obtained by photopolymerisation in the liquid crystalline state: synthesis and applications. Prog. Polym. Sci. Oxf **21**(6), 1165–1209 (1996)
53. Kelly, S.M.: Anisotropic networks, elastomers and gels. Liq. Cryst. **24**(1), 71–82 (1998)
54. Hikmet, R.A.M., Lub, J., Broer, D.J.: Anisotropic networks formed by photopolymerization of liquid-crystalline molecules. Adv. Mater. **3**(7–8), 392–394 (1991)
55. Broer, D.J., Boven, J., Mol, G.N., Challa, G.: In-situ photopolymerization of oriented liquid-crystalline acrylates, 3. Oriented polymer networks from a mesogenic diacrylate. Makromol. Chem. **190**, 2255–2268 (1989)
56. Kelly, S.M.: Anisotropic networks. J. Mater. Chem. **5**(12), 2047–2061 (1995)
57. McCulloch, I., Coelle, M., Genevicius, K., Hamilton, R., Heckmeier, M., Heeney, M., Kreouzis, T., Shkunov, M., Zhang, W.: Electrical properties of reactive liquid crystal semiconductors. Jpn. J. Appl. Phys. **47**(1 PART 2), 488–491 (2008)
58. McCulloch, I., Zhang, W., Heeney, M., Bailey, C., Giles, M., Graham, D., Shkunov, M., Sparrowe, D., Tierney, S.: Polymerisable liquid crystalline organic semiconductors and their fabrication in organic field effect transistors. J. Mater. Chem. **13**(10), 2436–2444 (2003)
59. Huisman, B.H., Valeton, J.J.P., Nijssen, W., Lub, J., Ten Hoeve, W.: Oligothiophene-based networks applied for field-effect transistors. Adv. Mater. **15**(23), 2002–2005 (2003)
60. Baldwin, R.J., Kreouzis, T., Shkunov, M., Heeney, M., Zhang, W., McCulloch, I.: A comprehensive study of the effect of reactive end groups on the charge carrier transport within polymerized and nonpolymerized liquid crystals. J. Appl. Phys. **101**(2) (2007)
61. Farrar, S.R., Contoret, A.E.A., O'Neill, M., Nicholls, J.E., Richards, G.J., Kelly, S.M.: Nondispersive hole transport of liquid crystalline glasses and a cross-linked network for organic electroluminescence. Phys. Rev. B **66**(12) (2002). doi:doi:12510710.1103/PhysRevB.66.125107
62. Hoang, M.H., Cho, M.J., Kim, D.C., Kim, K.H., Shin, J.W., Cho, M.Y., Js, J., Choi, D.H.: Photoreactive Ï€-conjugated star-shaped molecules for the organic field-effect transistor. Org. Electron. Phys. Mater. Appl. **10**(4), 607–617 (2009)
63. Arias, A.C., MacKenzie, J.D., McCulloch, I., Rivnay, J., Salleo, A.: Materials and applications for large area electronics: solution-based approaches. Chem. Rev. **110**(1), 3–24 (2010)
64. Tsao, H.N., Cho, D., Andreasen, J.W., Rouhanipour, A., Breiby, D.W., Pisula, W., Müllen, K.: The influence of morphology on high-performance polymer field-effect transistors. Adv. Mater. **21**(2), 209–212 (2009)
65. Zeng, L., Yan, F., Wei, S.K.H., Culligan, S.W., Chen, S.: Synthesis and processing of monodisperse oligo(fluorene-co-bithiophene)s into oriented films by thermal and solvent annealing. Adv. Funct. Mater. **19**(12), 1978–1986 (2009)